V European Conference on Computational Fluid Dynamics
ECCOMAS CFD 2010
J. C. F. Pereira and A. Sequeira (Eds)
Lisbon, Portugal, 14–17 June 2010

A CHARACTERISTIC-BASED SPLIT FINITE VOLUME ALGORITHM FOR THE SOLUTION OF INCOMPRESSIBLE FLOW PROBLEMS

Masoud Nickaeen*, Ali Ashrafizadeh†

*,† DOS Lab, K.N. Toosi University of Technology, Faculty of Mechanical Engineering,
No. 17, Pardis Street, Vanak Square, Postal Code: 19991 43344, Tehran, Iran.

* e-mail: nickaeen64@gmail.com

† e-mail: ashrafizadeh@kntu.ac.ir

Key words: Finite volume, Characteristic based split, Fully explicit, Local time stepping, Artificial compressibility.

Abstract. *The characteristic-based split (CBS) method has been widely used in the finite element community to facilitate the numerical modeling of the Navier-Stokes equations. In this paper a CBS-based finite volume algorithm is introduced for the solution of incompressible Navier-Stokes equations. The proposed method is implemented on a co-located grid arrangement and employs a transient fractional step method. In the first step, an explicit characteristic-based method is employed to obtain an intermediate velocity field from the modified momentum equations. Using continuity as an equation for pressure, the divergence-free velocity constraint of incompressible flow is also enforced in the second step. To devise a fully explicit algorithm for the solution of the pressure equation, an artificial compressibility factor is also defined and used. The correct, divergence-free velocity field is calculated afterwards using the intermediate velocities and the pressure field. Explicit time iterative solution of the finite volume algorithm discussed above is subjected to time step limitations. To validate the proposed CBS finite volume method, computational results are compared to those of numerical and experimental benchmark solutions. Satisfactory convergence rates and accurate results are obtained in all steady state and transient test cases.*

1 INTRODUCTION

Incompressible viscous flow phenomena arise in numerous disciplines in science and engineering. The behavior of flow in this case is mathematically expressed using well known Navier-Stokes (NS) equations. Numerical methods of incompressible Navier-Stokes equations (INSE) are major parts of the well-astablished yet rapidly growing field of computational fluid dynamics (CFD). CFD is now emerging as a necessary tool in the solution of science and engineering problems.

Numerical oscillations due to central difference approximation of the convective terms and the instabilities of the pressure field arising from inappropriate pressure-velocity coupling are two major obstacles in the numerical solution of INSEs, which are evidently common to all numerical solution techniques of these equations.

In the finite volume context, for instance, the central difference scheme, which is equivalent to standard finite element Galerkin method, produces unrealistic oscillations. This problem can be solved with up-winding strategies originally developed in the finite difference context. In the finite element framework, Petrov-Galerkin and Galerkin least square schemes[1] are solutions with similarities to those used in the finite volume community. Numerical schemes such as characteristic Galerkin or Taylor-Galerkin[1] are also two remedies to this long-standing problem.

In the present study a method similar to characteristic-Galerkin procedure is employed. We perform the temporal discretization of the modified momentum equations using the characteristic concept. This leads to the introduction of additional second order terms that prevent the numerical oscillations normally occurred with central approximation of convection terms in convection-dominated flows.

The characteristic-based split (CBS) algorithm is developed and used in the finite volume context. This algorithm is the extension of the general CBS method initially introduced by Zienkiewicz and Codina in a finite element framework[2]. The CBS finite volume scheme uses three steps to obtain pressure and velocity fields. The advantages of such a time stepping procedure include exploiting co-located grid arrangement and obtaining stable pressure solution. To devise a fully explicit algorithm, an artificial compressibility (AC) method is also employed. This AC method is a standard scheme based on the original work by Chorin[3].

Therefore a fully explicit CBS finite volume code combined with AC method is developed for the solution of incompressible flow problems. The unsteady flows can be solved via a dual time stepping procedure. Numerical simulations of two benchmark steady state problems and one transient problem are presented. The computational results are also compared to those of numerical or experimental solutions available in the literature.

2 FORMULATION AND DISCRITIZATION

2.1 Governing equations

The governing equations for the viscous incompressible flow can be written as follows:

Mass conservation:

$$\frac{\partial \rho}{\partial t} + \frac{\partial (U_i)}{\partial x_i} = 0 \tag{1}$$

In Eq. (1), $U_i = \rho u_i$ are components of the mass flux.

The transient density term in the continuity equation can be replaced by the following relation under isentropic flow assumption:

$$\frac{\partial \rho}{\partial t} = \frac{1}{c^2}\frac{\partial p}{\partial t} \tag{2}$$

where c is the wave speed.
Momentum conservation:

$$\frac{\partial (U_i)}{\partial t} + \frac{\partial (U_i u_j)}{\partial x_j} = -\frac{\partial p}{\partial x_i} + \mu \frac{\partial}{\partial x_j}\left(\frac{\partial u_i}{\partial x_j}\right) \tag{3}$$

In the above equations u_i is the velocity component, ρ is the density, p is the pressure and μ is the constant dynamic viscosity.

The non-dimensional variables are defined as follows:

$$\begin{gathered} x_i' = \frac{x_i}{L},\ u_i' = \frac{u_i}{u_\infty},\ t' = \frac{tu_\infty}{L} \\ p' = \frac{p}{\rho_\infty u_\infty^2},\ \rho' = \frac{\rho}{\rho_\infty},\ c'^2 = \frac{c^2}{u_\infty^2} \end{gathered} \tag{4}$$

where u_∞ is the free stream velocity, ρ_∞ is the free stream density and L is any relevant characteristic length.

The non-dimensional forms of the equations are then obtained as follows:

$$\frac{1}{c'^2}\frac{\partial p'}{\partial t'} + \frac{\partial (U_i')}{\partial x_i'} = 0 \tag{5}$$

$$\frac{\partial (U_i')}{\partial t'} + \frac{\partial (U_i' u_j')}{\partial x_j'} = -\frac{\partial p'}{\partial x_i'} + \frac{1}{\mathrm{Re}}\frac{\partial}{\partial x_j'}\left(\frac{\partial u_i'}{\partial x_j'}\right) \tag{6}$$

In the non-dimensional momentum equations, Re is the Reynolds number defined as:

$$\mathrm{Re} = \frac{Lu_\infty}{\nu}$$

where $\nu = \mu / \rho_\infty$ is the kinematic viscosity.

2.2 Characteristic-based split

The splitting process was initially introduced by Chorin[3] for incompressible flow problems in the finite difference framework. After that, a splitting method was developed in the finite element context and employed for different applications of incompressible flow[4,5,6]. However, the algorithm in its full form was first introduced in 1995 by Zienkiewicz and Codina[2] to solve the fluid dynamics equations of both compressible and incompressible flows. The foremost advantage of this method is the capability of solving either incompressible or compressible subsonic and supersonic flows by the same algorithm[1]. The CBS is developed here for the solution of INSEs in the finite volume context.

2.3 Temporal discretization

Using Eq. (6), the momentum equation can be written as follows[1] (primes are dropped from the non-dimensional equations for the sake of simplicity):

$$\frac{\partial(U_i)}{\partial t} + \frac{\partial\left(U_i u_j\right)}{\partial x_j} = \frac{1}{\mathrm{Re}}\frac{\partial}{\partial x_j}\left(\frac{\partial u_i}{\partial x_j}\right) + Q_i^{n+\theta_2} \tag{7}$$

The $Q_i^{n+\theta_2}$ is a known quantity at $t = t^n + \theta_2 \Delta t$ and is

$$\begin{aligned} Q_i^{n+\theta_2} &= -\frac{\partial p^{n+\theta_2}}{\partial x_i} = -\left(\frac{\partial p^n}{\partial x_i} + \theta_2 \frac{\partial \Delta p}{\partial x_i}\right) \\ \Delta p &= p^{n+1} - p^n \end{aligned} \tag{8}$$

Using the explicit characteristic method[1], Eq. (7) can be written as follows:

$$\begin{aligned} U_i^{n+1} - U_i^n &= \Delta t\left[-\frac{\partial\left(U_i u_j\right)}{\partial x_j} + \frac{1}{\mathrm{Re}}\frac{\partial}{\partial x_j}\left(\frac{\partial(u_i)}{\partial x_j}\right)\right]^n \\ &+ \frac{\Delta t^2}{2} u_k \frac{\partial}{\partial x_k}\left[\frac{\partial\left(U_i u_j\right)}{\partial x_j} - \frac{1}{\mathrm{Re}}\frac{\partial}{\partial x_j}\left(\frac{\partial(u_i)}{\partial x_j}\right)\right]^n + \Delta t Q_i^{n+\theta_2} - \frac{\Delta t^2}{2} u_k \frac{\partial}{\partial x_k}\left(Q_i^n\right) \end{aligned} \tag{9}$$

Comparing the above equation with Eq. (7), some additional second-order terms are added to the original momentum equation. These terms act as a smoothing operator that reduces the oscillations arising from the spatial discretization of the convection terms. In other words, in the new form of the momentum equation the spatial discretization of the convection terms can be carried out using the central difference scheme without having numerical oscillations in high Reynolds number flows. This is due to the stabilization nature of the additional diffusion terms arising from discretization along the characteristic lines.

Choosing different values of θ_2, Eq. (9) can be formulated in explicit and semi-implicit forms. In the present work, with $\theta_2 = 0$ the fully explicit form is employed.

At this stage two different splitting procedures can be used to implement the fractional step method[1]. In this paper split A is used, in which the pressure gradient is removed from Eq. (9) and an intermediate velocity U_i^* is defined as follows[1]:

$$\begin{aligned} U_i^* - U_i^n &= \Delta t\left[-\frac{\partial\left(U_i u_j\right)}{\partial x_j} + \frac{1}{\mathrm{Re}}\frac{\partial}{\partial x_j}\left(\frac{\partial u_i}{\partial x_j}\right)\right]^n \\ &+ \frac{\Delta t^2}{2} u_k \frac{\partial}{\partial x_k}\left[\frac{\partial\left(U_i u_j\right)}{\partial x_j} - \frac{1}{\mathrm{Re}}\frac{\partial}{\partial x_j}\left(\frac{\partial u_i}{\partial x_j}\right)\right]^n \end{aligned} \tag{10}$$

This equation will be solved subsequently by an explicit time step applies to the discretized form. The correction given below is available once the pressure increment is evaluated:

$$\Delta U_i = U_i^{n+1} - U_i^* = -\Delta t \frac{\partial p^n}{\partial x_i} + \frac{\Delta t^2}{2} u_k \frac{\partial}{\partial x_k}\left(\frac{\partial p^n}{\partial x_i}\right) \tag{11}$$

Enforcing the continuity equation, Eq. (5) can be written as follows:

$$\left[\frac{1}{c^2}\right]\left(p^{n+1}-p^n\right)=-\Delta t\,\frac{\partial U_i^{n+\theta_1}}{\partial x_i}=-\Delta t\left[\frac{\partial U_i^n}{\partial x_i}+\theta_1\frac{\partial \Delta U_i}{\partial x_i}\right] \tag{12}$$

where $\Delta U_i = U_i^{n+1} - U_i^n$.

Replacing U_i^{n+1} from Eq. (11) and neglecting higher-order pressure terms, we have

$$\left[\frac{1}{c^2}\right]\left(p^{n+1}-p^n\right)=-\Delta t\left[\theta_1\frac{\partial U_i^*}{\partial x_i}+\left(1-\theta_1\right)\frac{\partial U_i^n}{\partial x_i}\right]+\Delta t^2\theta_1\frac{\partial}{\partial x_i}\left(\frac{\partial p^n}{\partial x_i}\right) \tag{13}$$

with $0.5<\theta_1<1$.

In summary, the three steps of the fully explicit CBS scheme are:

1. Solve Eq. (10) for U_i^*
2. Solve Eq. (13), for p^{n+1}
3. Solve Eq. (11) for U_i^{n+1}

The semi-discrete equations of (10, 11 and 13) can be solved after carrying out the finite volume spatial discretization.

2.4 Artificial compressibility (AC) method

The incompressible flow solvers are generally classified into projection or velocity correction and AC schemes by many authors. An efficient algorithm that employs good features from both classifications was first introduced by Nithiarasu[7] as an extension to the general CBS method in the finite element context. In the Present work, a finite volume algorithm based on the work of Nithiarasu[7] is presented. In this section, the AC parameter and local time step calculations are explained.

The compressible wave speed in Eq. (13) approaches infinity for incompressible flow problems. This prevents the explicit treatment of the pressure equation. To devise a fully explicit algorithm, the wave speed can be replaced by an appropriate local artificial parameter β. It is essential to define a β which is suitable for different Reynolds numbers and also for different flow regimes of a specific problem.

In this work, the following relations are considered for the artificial wave speed β and for the local time step Δt [7]

$$\beta=\max(\varepsilon, v_{conv}, v_{diff}) \tag{14}$$

where ε is a constant (taken as 0.5 here), v_{conv} and v_{diff} are the convective and diffusion velocities, respectively. These velocities are calculated as follows:

$$\begin{aligned} v_{conv} &= \sqrt{u_i u_i} \\ v_{diff} &= \frac{2}{h\,\mathrm{Re}} \end{aligned} \tag{15}$$

In the above equation, h is a non-dimensional control volume length scale. In a two dimensional uniform grid, h is simply the width of the control volume. In non-uniform grids; however, different length scales can be used.

The critical time step is calculated as follows:

$$\Delta t=\min\left(\Delta t_{conv}, \Delta t_{diff}\right) \tag{16}$$

where

$$\Delta t_{conv} = \frac{h}{u_{conv} + \beta} \tag{17}$$

and

$$\Delta t_{diff} = \frac{h^2 \operatorname{Re}}{2} \tag{18}$$

To ensure the stability of the method, the final local time step is chosen as a fraction of the critical time step. In other words, a safety factor varying between 0 and 1 is imposed on the calculated time step.

2.5 Spatial discretization via FVM

2.5.1. Co-located grid

To start the finite volume spatial discretization, solution domain must be divided into control volumes. In this study a co-located, structured grid is used in a Cartesian coordinate system. The computational grid is generated based on the cell-centered scheme and employs common finite volume notations. An example of a grid generated in a rectangular domain is shows in Fig. 1.

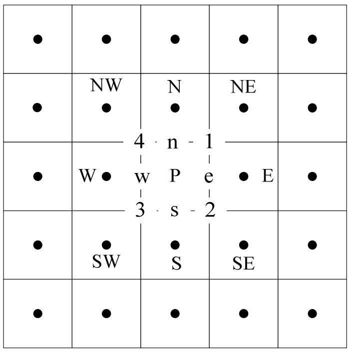

Figure 1: A cell-centered finite volume grid.

In Fig. 1, capital and small letters represent the control volume centers and the Integration Points (IP), respectively. Numbers from 1 to 4 are the four corners of a typical control volume.

2.5.2. Finite volume discretization: step 1

To carry out the first discretization step of the AC-CBS scheme, we integrate Eq. (10) over a control volume $\forall p$ associated with cell p shown in Fig. 1. Using the Divergence theorem, the volume integrals change to surface integrals and this introduces the IP approximations into the equation. For example, the spatial semi-discrete form of the convection terms in the x-momentum equation (i=1 in Eq. (10)) is written as follows:

$$\begin{aligned}
&\int_{\forall_p} \frac{\partial \left(U_i u_j\right)^n}{\partial x_j} d\forall_p = \\
&\int_{\forall_p} \left[\frac{\partial (Uu)^n}{\partial x} + \frac{\partial (Uv)^n}{\partial y} \right] d\forall_p = \Delta y_p \left[(Uu)_e - (Uu)_w \right]^n + \Delta x_p \left[(Uv)_n - (Uv)_s \right]^n
\end{aligned} \tag{19}$$

The IP velocities are related to nodal values via linear approximation. For example, the velocity on the right face of the cell p is approximated as follows:

$$u_e = \frac{\dfrac{u_P}{\Delta x_P} + \dfrac{u_E}{\Delta x_E}}{\dfrac{1}{\Delta x_P} + \dfrac{1}{\Delta x_E}} \tag{20}$$

In Eq. (19), Δx and Δy represent the cell-face areas in Fig. 1. All other IP values are treated similarly.

To complete the first step of the discretization procedure, we have to approximate the diffusion fluxes. These fluxes are also approximated using the central difference scheme. Note that the discretization of additional diffusion terms needs the values of the velocities at the control volume corners. These corner values are approximated using the weighted average of the surrounding nodal values. For example, the x-velocity of point 1 in Fig. 1 is approximated as follows:

$$u_1 = \frac{\dfrac{u_N}{\forall_N} + \dfrac{u_{NE}}{\forall_{NE}} + \dfrac{u_E}{\forall_E} + \dfrac{u_P}{\forall_P}}{\dfrac{1}{\forall_N} + \dfrac{1}{\forall_{NE}} + \dfrac{1}{\forall_E} + \dfrac{1}{\forall_P}} \tag{21}$$

The discretization procedure yields a fully explicit equation relating the cell-centered value of intermediate velocities to that of the cell-centered velocities and their neighbors (*E, W, N, S, NE, NW, SE* and *SW* in Fig. 1) from the previous time step.

2.5.3. Finite volume discretization: step 2

In the second step of the AC-CBS method, pressure is obtained from Eq. (13). As mentioned before, for incompressible flow problems, the wave speed *c* is replaced with the artificial parameter β calculated from Eq. (14). Thus, the final form of the pressure equation for $\theta_2 = 0$ is obtained as follows:

$$\left[\frac{1}{\beta^2}\right]\left(p^{n+1} - p^n\right) = -\Delta t \left[\theta_1 \frac{\partial U_i^*}{\partial x_i} + \left(1 - \theta_1\right) \frac{\partial U_i^n}{\partial x_i} \right] + \Delta t^2 \theta_1 \frac{\partial}{\partial x_i} \left(\frac{\partial p^n}{\partial x_i} \right) \tag{22}$$

The finite volume discretization of this equation is simple. Again, after integrating over control volumes and introducing the surface integrals into the equation, the central difference scheme is used to discretize pressure gradients on the IPs. Solution of this equation is done with an explicit procedure.

2.5.4. Finite volume discretization: step 3

The correct divergence-free velocities are calculated from Eq. (11). Neglecting higher order pressure terms of this equation, the final velocities are calculated from the following equation:

$$\Delta U_i = U_i^{n+1} - U_i^* = -\Delta t \frac{\partial p^n}{\partial x_i} \tag{23}$$

From Steps 1 and 2 we have the intermediate velocities and the pressure, respectively. Using these values after integrating the above equation over the control volumes, the final correct velocities can be easily obtained. Explicit solution of this equation is carried out to obtain the final velocities.

2.6 Boundary conditions

The main obstacle in the imposition of proper boundary conditions in INSEs is the lack of an independent equation for pressure.

In the present study, the Dirichlet and Neumann velocity boundary conditions are applied in the first step of the algorithm. Thus, the velocity boundary conditions have been used to obtain intermediate velocities as well. Since the cell-centered grid is employed, the required pressure values on the control surfaces are estimated using linear extrapolation from the old values of inner nodes.

Solution of the second step requires implementation of appropriate pressure boundary conditions. In the case of known pressure values on the boundary, the implementation is simple and straightforward. In other cases with velocities or their gradients as known boundary conditions, the proper boundary condition for the pressure equation is applied using velocity components normal to the physical boundary of interest.

In the third step, the extrapolated values of IP pressures of the first step are again used to obtain the correct velocities.

3 RECOVERING REAL TRANSIENT SOLUTION

The principle of recovering the transient solution in the AC method is explained in some studies[8,9]. In this work, a dual time steeping method described by Nithiarasu[7] is employed to obtain accurate transient solutions from the proposed fully explicit AC-CBS finite volume algorithm.

The time step Δt appeared in the previous sections, accelerate solution to steady state. This pseudo-time step is calculated locally and is subjected to stability conditions of equations (16-18). The addition of a transient term to the momentum equations introduces several steady state problems that must be converged to a prescribed pressure residual within each real time step.

The CBS procedure supports two approaches for the addition of the real transient terms to the momentum equations[7]. In this study the real transient term is added to the third step of the algorithm where the final divergence free velocities are calculated. After the addition of the real transient terms to the Eq. (23) the modified equation, being used as the third step in the CBS algorithm, is as follows:

$$\Delta U_i = U_i^{n+1} - U_i^* = -\Delta t \frac{\partial p^n}{\partial x_i} - \Delta t \frac{\Delta U_{i,\tau}}{\Delta \tau} \tag{24}$$

where $\Delta\tau$ is the real time step. The $\Delta U_{i,\tau}$ is defined here using a second-order approximation as follows:

$$\frac{\Delta U_{i,\tau}}{\Delta\tau} = \frac{3U_i^{n+1} - 4U_i^n + U_i^{n-1}}{2} \tag{25}$$

In the above equation U_i^n and U_i^{n-1} are the velocities from the previous real time steps that must be stored at the start of each real time step.

4 RESULTS AND DISCUSSION

The performance of the proposed fully explicit AC-CBS finite volume scheme is investigated in this part. This algorithm is capable of solving two dimensional transient INSEs. To validate the method, two steady state benchmark problems have been studied and compared with the available numerical and experimental works in the literature. The transient performance of the solution code is also investigated by comparing the results with previous numerical works in the literature.

4.1 The lid-driven cavity steady test case

As the first test case, the lid-driven cavity flow in a $[0,1]\times[0,1]$ square as shown in Fig. 2 is studied here. This is a well known benchmark problem normally used to evaluate the performance of the incompressible flow solvers.

In this work, two different non-uniform structured meshes, shown in Fig. 3, are employed to solve the lid-driven cavity problem. The mesh 1 is a 85×85 computational grid (Fig. 3(a)) and mesh 2 is a 125×125 grid (Fig. 3(b)).

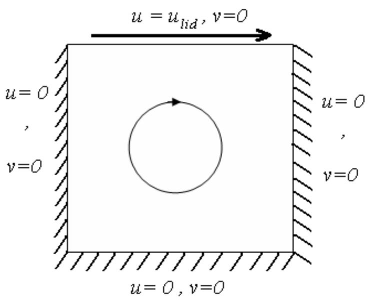

Figure 2: The lid-driven cavity test case.

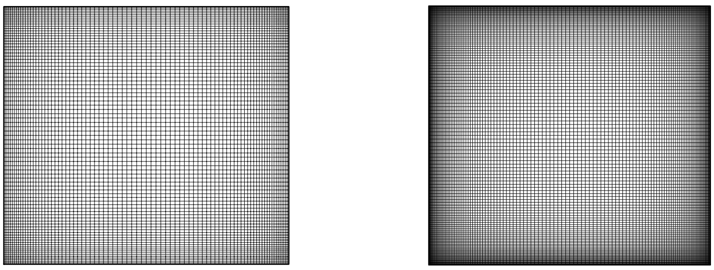

(a) Mesh 1 (b) Mesh 2

Figure 3: (a) Mesh 1, 85×85; (b) Mesh 2, 125×125

Mesh 1 is used to solve the cavity flow in Reynolds numbers 400 and 1000. In Figs. 4 and 5, the velocity distributions at various Reynolds numbers are compared with the benchmark solution of Ghia *et al.*[10]. The vertical velocity (v) components along the mid-horizontal line are compared in Fig. 4 and the horizontal velocity (u) components along the mid-vertical line are compared in Fig. 5. The computational results of fully explicit AC-CBS finite volume method are in close agreement with the benchmark solution.

To obtain accurate numerical results for high Reynolds number 5000, mesh 2 is used. Again in this case the horizontal and vertical mid-plane velocities are compared with those of Ghia *et al.*[10]. Figure 6 shows good agreement between the results of the present method and those of Ghia[10].

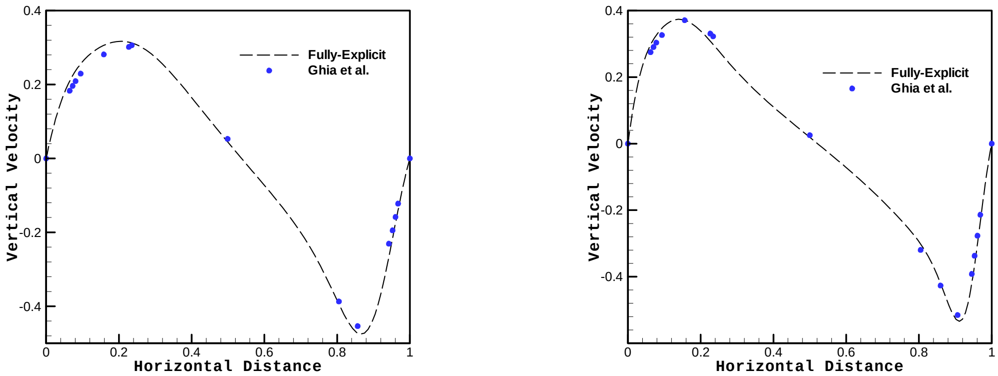

(a) (b)

Figure 4: Lid-driven cavity flow, comparison with Ghia *et al.*[10] for the v velocity profile along the horizontal center line (a) Reynolds = 400; (b) Reynolds = 1000.

4.2 The backward facing step steady test case

In the second test case, backward facing step flow, shown in Fig. 7, is studied. It is a 2D channel flow with the inlet width h and the outlet width H. The length of the flow passage is equal to 26H. Depending on the Value of the flow Reynolds number, different recirculation zones occur in the flow as shown schematically in Fig. 7.

In this problem, a fully-developed parabolic u-velocity profile is prescribed at the inlet of the channel and zero-normal velocity derivatives are imposed at the exit. The location of the outflow boundary is chosen to be sufficiently far downstream of the step so that it does not affect the position of the recirculation zones. All other walls are subjected to the no-slip boundary condition.

To compare the computational results with the experimental results of Armaly et al.[11], the expansion ratio $E = H/h$ is set to be 1.94.

A uniform structured mesh is employed here to investigate the reattachment and separation lengths for Reynolds numbers from 100 to 800. This mesh is composed of two blocks, block 1 with 60×30 control volumes in the inlet channel before the step and block 2 with 200×60 control volumes in the zone downstream of the step.

Computed non-dimensionalised separation and reattachment lengths against inlet Reynolds number are shown in Fig. 8 together with the experimental data presented by Armaly *et al.*[11]. The computational results of the fully explicit AC-CBS finite volume method are in close agreement with the experimental results up to Reynolds 500. For flows with the Reynolds number above 500, the reattachment and the separation length X_2 deviate from the experimental results. These deviations for the Reynolds number above 500 are probably due to the three-dimensional effects that are neglected in the present 2D analysis.

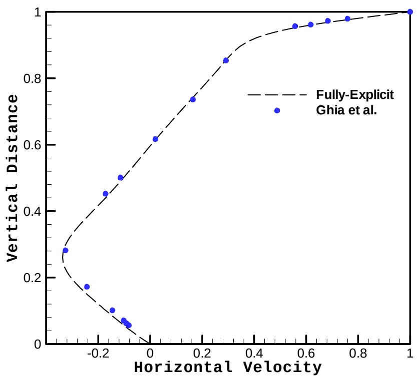

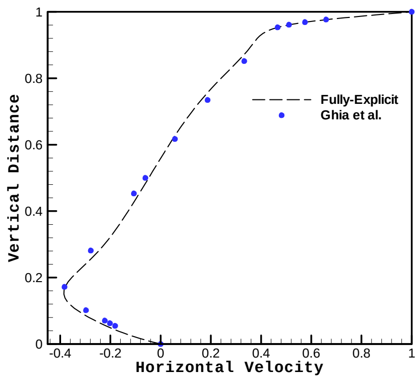

(a) (b)

Figure 5: Lid-driven cavity flow, comparison with Ghia *et al.*[10] for the *u* velocity profile along the vertical center line (a) Reynolds = 400; (b) Reynolds = 1000

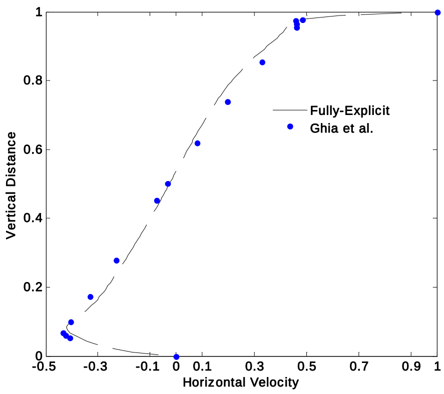

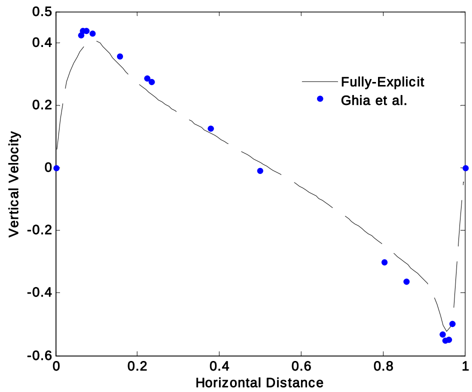

(a) (b)

Figure 6: Lid-driven cavity flow at Reynolds = 5000 on mesh 2, comparison with Ghia *et al.*[10] of velocity profiles along the center lines (a) *u* velocity profile; (b) *v* velocity profile

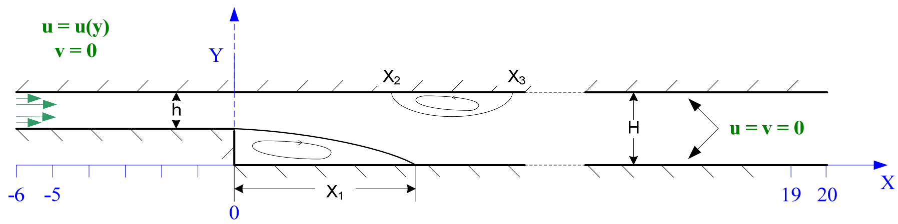

Figure 7: Backward facing step flow, geometry and boundary conditions

4.3 The lid-driven cavity transient test case

To investigate the accuracy of the transient solutions, the lid-driven cavity flow is again considered here. The flow geometry and boundary conditions are the same as the steady state problem studied above. The transient solution is started with the fluid at rest in the domain as the initial condition.

As the first attempt, mesh 1 is used to solve the transient flow with Reynolds numbers 400 and 1000 to reach the steady state. The appropriate results are shown in Fig. 9. In Fig. 9(a), the center line *v*-velocity profile at Reynolds 400 is shown in different times of the transient solution and the final steady state profile is compared to that of Ghia *et al.*[11] These calculations are repeated for Reynolds 1000 in Fig. 9(b). Again in this case the steady state result is successfully compared to the results of Ghia *et al.*[11]. The results show that the dual time stepping procedure in combination with the proposed AC-CBS finite volume method works well for the solution of transient flows.

To verify the transient results, the transient lid-driven cavity flow for two Reynolds numbers 400 and 1000 is studied using mesh 1. Transient solution of the *u*-velocity component at the center of the cavity is plotted in Fig. 10(a) for Reynolds 400 and in Fig. 10(b) for Reynolds 1000. The results are in good agreement with those of Wirogo[12]. The difference between the minimum values in transient history profiles of Reynolds 1000 is due to mesh resolution used here as compared with Wirogo[12].

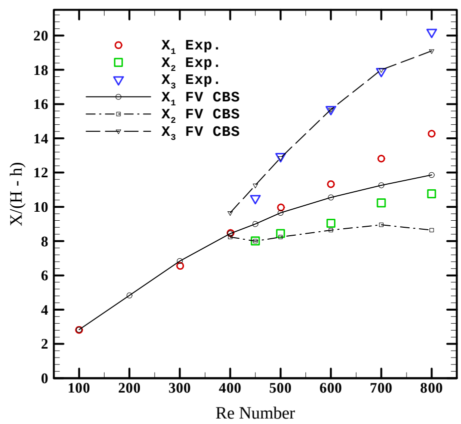

Figure 8: Backward facing step flow, variation in reattachment and separation lengths with Reynolds number and comparison with experimental results[11]

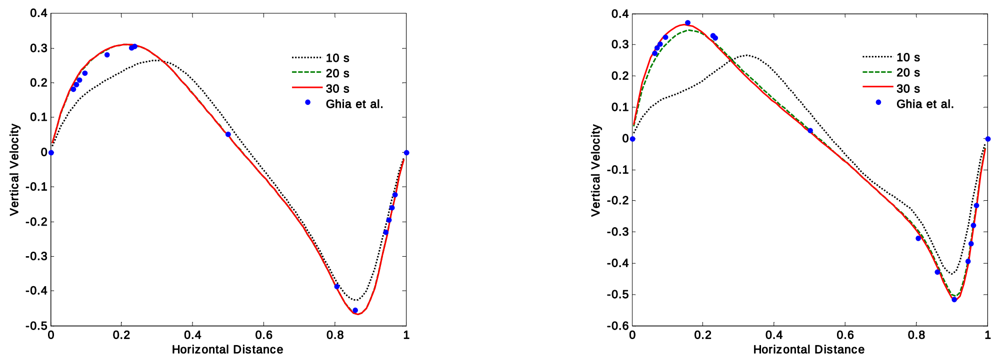

(a) (b)

Figure 9: Lid-driven cavity transient flow on mesh 1, comparison with Ghia *et al.*[10] of *v* velocity profiles along the center line at different times (a) Reynolds 400; (b) Reynolds 1000

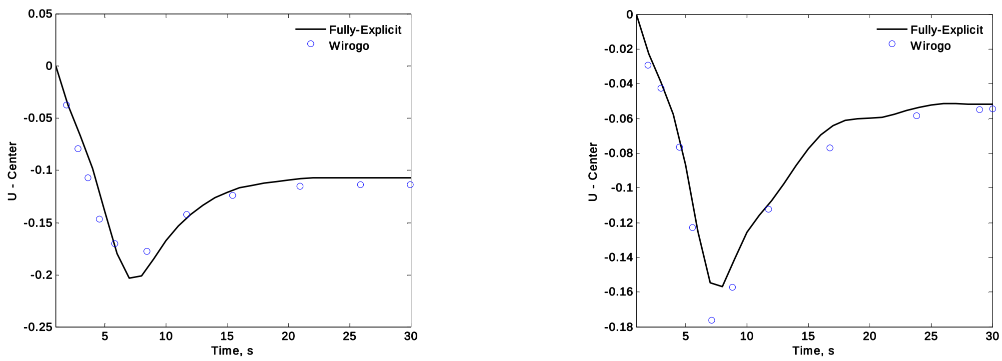

(a) (b)

Figure 10: Transient solution of *u* velocity at the center of cavity, solution on mesh 1 and comparison with Wirogo[11] (a) Reynolds 400; (b) Reynolds 1000

5 CONCLUSIONS

In this work, an artificial compressibility CBS finite volume algorithm is proposed and successfully employed for the solution of INSEs. The fully explicit algorithm is capable of solving steady state incompressible flow problems up to high Reynolds numbers with excellent accuracy. The main advantage of the proposed method is the ability to solve the NS equations in the fully explicit, matrix free form.

To recover real time solutions in transient flow problems, a dual time stepping method is also employed. The results show that the dual time stepping procedure in combination with the proposed AC-CBS finite volume method, works well for the solution of transient incompressible flows.

REFERENCES

[1] O. C. Zienkiewicz, R. L. Taylor and P. Nithiarasu, The Finite Element Method for Fluid Dynamics, *Butterworth and Heinemann*, 6th edition (2005).

[2] O.C. Zienkiewicz and R. Codina, A general algorithm for compressible and incompressible flow, Part I. The split characteristic based scheme, *Int. J. Num. Meth. Fluids*, 20, 869-85 (1995).

[3] A. J. Chorin, Numerical solution of Navier–Stokes equations, *Mathematics of Computation,* 22, 745–762, (1968).

[4] G. Comini, S. Del Guidice, Finite element solution of incompressible Navier–Stokes equations, *Numerical Heat Transfer*, Part A, 5, 463–478 (1972).

[5] M. Kawahara, K. Ohmiya, Finite element analysis of density flow using the velocity correction method, *Int. J. Num. Meth in Fluids,* 5, 981–993 (1985).

[6] B. Ramaswamy, T. C. Jue and J.E. Akin, Semi-implicit and explicit finite element schemes for coupled fluid thermal problems, *International J. for Num. Meth. in Eng.*, 34, 675–696 (1992).

[7] P. Nithiarasu, An efficient artificial compressibility (AC) scheme based on the characteristic based split (CBS) method for incompressible flows, *Int. J. Numer. Methods Engrg.*, 56, 1815–1845 (2003).

[8] A.G. Malan, R.W. Lewis and P. Nithiarasu, An improved unsteady, unstructured, artificial compressibility, finite Volume scheme for viscous incompressible flows: Part I. Theory and implementation, *Int. J. Numer. Methods Engrg.*, 54, 695–714 (2002).

[9] AL. Gaitonde, A dual time method for two dimensional incompressible flow calculations, *Int. J. Numer. Methods Engrg.,* 41, 1153–1166 (1998).

[10] U. Ghia, K.N. Ghia and C.T. Shin, High-resolution for incompressible flow using the Navier–Stokes equations and multigrid method, *J. Comp. Phys.*, 48, 387–411 (1982).

[11] B. F. Armaly, F. Durst, J. C. F. Pereira and B. Schönung, Experimental and theoretical investigation of backward-facing step flow, *J. Fluid Mech.*, 127, 473-496 (1983).

[12] S. Wirogo, Flux Corrected Method: An Accurate Approach to Fluid Flow Modeling, PhD thesis, Iowa State University, Ames (1997).